COO-1195-273

CONF-730943--6

A_1, A_2, and A_3 PRODUCTION IN $\pi^- p \to \pi^- \pi^- \pi^+ p$ AT 25 AND 40 GeV/c

Yu.M. Antipov*), G. Ascoli**), R. Busnello***),
M.N. Kienzle-Focacci***), W. Kienzle†), R. Klanner††),
A.A. Lebedev*), P. Lecomte***), V. Roinishvili†††),
A. Weitsch×) and F.A. Yotch*)

CERN-IHEP Boson Spectrometer

(Joint Experiment of the
Institute of High-Energy Physics, Serpukhov, USSR, and the
European Organization for Nuclear Research, Geneva, Switzerland)

ABSTRACT

A sample of ∿ 70,000 fitted events of the reaction $\pi^- p \to \pi^- \pi^- \pi^+ p$ at 25 and 40 GeV/c has been obtained with the CERN-IHEP Boson Spectrometer at the Serpukhov Accelerator. A partial-wave analysis shows that:

i) A_1 and A_3 cannot be described by a Breit-Wigner amplitude;

ii) the A_2 can be well described by a Breit-Wigner amplitude;

iii) although A_1, A_3, and A_2 have different properties, the energy dependence of their production cross-section is similar.

MASTER

Submitted to the
2nd Aix-en-Provence International Conference
on Elementary Particles, September 1973

*) IHEP, Serpukhov, USSR.

**) University of Illinois, Urbana, Ill., USA.

***) University of Geneva, Geneva, Switzerland.

†) CERN, Geneva, Switzerland.

††) University of Munich, Munich, Germany.

†††) Institute of Physics, Tbilisi, USSR.

×) University of Munich, now at Stanford Linear Accelerator Center, Calif., USA.

1. INTRODUCTION

The reaction $\pi^- p \to \pi^- \pi^- \pi^+ p$ has been measured at 25 and 40 GeV/c with the CERN-IHEP Boson Spectrometer at the Proton Accelerator at Serpukhov. We discussed in previous publications[1,2] how the data were obtained and analysed, as well as the general features of the reaction analysed by the partial-wave method[3,4]. Here we present results about production and decay of the three spin-parity (J^P) states which dominate the 3π system below 2 GeV:

the 1^+ state, known as the A_1 system,
the 2^+ state, known as the A_2 system,
the 2^- state, known as the A_3 system.

We emphasize the fact that most of the results shown below are based on two samples of data at p_{lab} = 25 and 40 GeV obtained by superposing data from runs covering different t-intervals (see Table 1 of Ref. 1). For the study of t-dependence we use instead the result of a single run at 25 GeV/c $[|t| = 0.10\text{-}0.22\ (\text{GeV/c})^2]$ and a single run at 40 GeV/c $[|t| = 0.04\text{-}0.33\ (\text{GeV/c})^2]$.

2. THE A_1 SYSTEM

2.1 Mass, width, and differential cross-section

We define the A_1 system as the 1^+ state which decays via S-wave into a ρ meson and a π meson (1^+S in our notation), and dominates the 3π system below 1.4 GeV. Figures 1a, 1b, and 1c show the 3π mass dependence of this state for the data measured at 25 and 40 GeV/c as well as for the combined data. The mass of the object is roughly 1150 MeV, its width about 300 MeV. In trying to get more accurate values for width and mass of the A_1, one finds that the slope of the differential cross-section for A_1 production $[d\sigma/dt \propto \exp(bt)]$ depends strongly on 3π mass. As we see from Table 1 and Fig. 2 it decreases from $\sim 12\ (\text{GeV/c})^{-2}$ to $\sim 7.5\ (\text{GeV/c})^{-2}$ between 1.0 and 1.4 GeV. As a result, the mass and the width of the A_1 system depend on the momentum transfer interval selected and their unique determination is thus impossible. In Table 1 we also list the integrated cross-section for the reaction

$$\pi^- p \to A_1^- p, \quad A_1^- \to \rho^0 \pi^-$$

obtained by extrapolating the exp (bt) dependence of the differential cross-section in the 3π mass intervals 1.0-1.2 GeV and 1.2-1.4 GeV.

2.2 Interference with other partial waves and resonance interpretation

The A_1 interferes strongly with all other partial waves of the 3π system. The partial-wave method thus allows us to determine the mass dependence of the relative phase between A_1 and the other partial waves. The phase difference between the production amplitudes for two partial waves a,b is given by the phase of the off-diagonal element of the 3π density matrix[1]:

$$\phi_{ab} = \arg(\rho_{ab}) .$$

If partial wave a corresponds to a resonance, which can be described by a Breit-Wigner amplitude (BW_a), and b does not, the phase is expected to be

$$\phi_{ab} = \phi_0 + \arg(BW_a) ,$$

where ϕ_0 is constant or a slowly varying function of $m_{3\pi}$. From Fig. 1 one sees that the intensities of the dominant background waves (0^-S, 1^+P, 2^-P) are slowly varying over the A_1 peak. We therefore expect that they provide reference phases to measure the A_1 phase. If the A_1 is a usual Breit-Wigner resonance we expect its phase to increase by 90° over one full width. From Fig. 1 we find that none of the interference phases shows this behaviour. We thus conclude that the total 1^+S state cannot be described by a simple Breit-Wigner amplitude.

It may be useful to comment on the limits that our results place on the production of a real, narrow A_1 resonance (A_1^R, $J^P = 1^+$, decay to $\rho^0\pi^-$) in addition to the broad 1^+ ($S \to \rho\pi$) effect (A_1^B). We quote three crude upper limits ($\sim$ 95% confidence level) on the cross-section $\pi^- p \to A_1^R p (A_1^R \to \rho^0\pi^-)$ at p_{lab} = 25-40 GeV/c, obtained from Fig. 1c under different assumptions regarding the production and decay of A_1^R:

a) A_1^R decays by s-wave, A_1^R and A_1^B are coherently produced: $\sigma(A_1^R \to \rho^0\pi^-) \lesssim 0.2$ μb;

b) A_1^R decays by s-wave, A_1^R and A_1^B are incoherently produced: $\sigma(A_1^R \to \rho^0\pi^-) \lesssim 5$ μb;

c) A_1^R decays by d-wave: $\sigma(A_1^R \to \rho^0\pi^-) \lesssim 0.3$ μb.

2.3 Polarization

With the partial-wave method we also determine the polarization density matrix of the A_1 system in the Gottfried-Jackson system*). Table 2 shows the results for the 25 GeV/c and 40 GeV/c data in the mass bin 1.0-1.2 GeV. The element ρ_{00} dominates, being about 0.95. The element combination $(\rho_{11} + \rho_{1-1})$, which corresponds to unnatural parity exchange[1)] is compatible with zero. The interference element between the M = 0 and |M| = 1 components ρ_{01} is real, and is compatible with the maximum value allowed by the positivity condition of the density matrix. This implies that the A_1 is produced in a pure M = 0 state, in a system which can be reached from the Gottfried-Jackson system by a rotation of the angle θ around the normal to the production plane. Figures 3a and 3b show how θ depends on momentum transfer and 3π mass. The value of θ is close to $10(\pm 3)^\circ$, which indicates a small but significant deviation from t-channel helicity conservation.

3. THE A_2 SYSTEM

We define the A_2 as the 2^+ state, which decays via d-wave into $\rho\pi$ (2^+D in our notation) and peaks around 1.3 GeV with a full width of roughly 100 MeV. We notice that it is the only state with different naturality[1)] $[P(-1)^J]$ from the incident π meson, which is strongly produced in the reaction $\pi^- p \to \pi^-\pi^-\pi^+ p$. Figure 4a shows the mass dependence of the 2^+D state. A fit of a relativistic d-wave Breit-Wigner**) without background to the data, yields the values for mass and width of the A_2:

$$M_{A_2} = 1315 \pm 5 \text{ MeV}, \quad \Gamma_{A_2} = 115 \pm 15 \text{ MeV}.$$

The result of the fit is drawn as a solid line in Fig. 4a. Figure 4b shows the dependence of the interference phase between the 2^+D state and the 1^+S state (and the 1^+P state) on 3π mass. The solid line is the variation we expect from the phase of a Breit-Wigner amplitude for the A_2

---

*) As discussed in Ref. 1, we assume the same polarization for both $1^+S(\rho\pi)$ and $1^+P(\varepsilon\pi)$ waves.

**) We use the parametrization:

$$BW(m) = \frac{m \cdot M_{A_2} \cdot \Gamma(m)}{\left[(m^2 - M_{A_2}^2)^2 + M_{A_2}^2 \Gamma^2(m)\right]}$$

$$\Gamma(m) = \Gamma_{A_2} (q/q_0)^5.$$

assuming constant phases for the 1^+ waves. The rapid increase of 90° over one full width of the A_2 peak is clearly seen in the data, and we thus conclude that the 2^+D state resonates at the A_2 mass.

In Fig. 5 we show the differential cross-section for the reaction

$$\pi^- p \to A_2^- p$$
$$\quad\quad \hookrightarrow \rho^0 \pi^-$$

in the mass interval between 1.2-1.4 GeV. In the 40 GeV/c data which cover the momentum transfer interval 0.04 to 0.33 $(\mathrm{GeV/c})^2$ there is a significant dip towards small $|t|$ values. The parametrization

$$\frac{d\sigma}{dt} \propto |t| \; e^{bt}$$

describes the data well and we obtain the parameters listed in Table 3. Integration over the full t-range gives the total cross-section $\sigma(A_2)$.

Table 4 lists the density matrix elements for A_2 production. The combination $\rho_{11} + \rho_{1-1}$, which is the $|M| = 1$ state produced by natural parity exchange, dominates and is close to one. All combinations which can be produced by unnatural parity exchange are zero within the statistical sensitivity of the data. For comparison we also quote the matrix elements obtained from the $\eta^0\pi^-$ decay mode at 40 GeV/c, where the A_2 signal appears with very little background[5].

4. THE A_3 REGION

In this paragraph we discuss the partial-wave analysis in the 3π mass interval 1.5-2.0 GeV. We concentrate on the 40 GeV/c data, for which the average acceptance of the magnetic spectrometer is 0.7 in the A_3 region (see Fig. 1 of Ref. 2). (The acceptance for our 25 GeV data is about 0.3 only and the statistical sensitivity of these data is lower. We note, however, that they show within errors the same features as the 40 GeV/C data.)

A difficulty of the partial-wave analysis of the A_3 region is that the number of weak but significant partial waves is large; it is therefore difficult to vary them all simultaneously. Our procedure is therefore to ask the following specific questions, and to see how stable the answers are when different sets of partial waves are chosen:

i) which partial wave is responsible for the A_3 enhancement?

ii) is the A_3 a resonance?

iii) what are its production parameters (cross-section, polarization)?

iv) are there candidates for further resonances in the interval 1.5-2.0 GeV?

The data have been analysed using several different sets of partial waves. The results shown in Fig. 6 were obtained using the two sets listed in Table 5. In both sets we restrict the polarizations to states:

$$|J^P 0\rangle \text{ for } J^P = 0^-, 1^+, \ldots \text{ and } |J^P\rangle + |J^P{-1}\rangle \text{ for } J^P = 1^-, 2^+, \ldots .$$

The choice is based on the results obtained in $m_{3\pi}$ = 1.0-1.4 GeV in this experiment and in $m_{3\pi}$ = 1.5-1.8 GeV in bubble chamber data (Ref. 4). Set I is the set used in Ref. 4. Set II includes systematically all partial waves with $\ell = 0,1,2$, for $\varepsilon\pi$ and $\rho\pi$ decay and $\ell = 0,1$ for $f\pi$ decay. In addition, set II includes the partial wave $3^+(D \to f\pi)$.

A comparison of the result of the fit (Hypothesis I) with the data is shown in Figs. 7 and 8. We find that the fit describes the data well.

In Fig. 6 we note the following features:

- The main partial waves [i.e. $0^-S(\varepsilon\pi)$, $1^+S(\rho\pi)$, $2^-S(f\pi)$, $2^-P(\rho\pi)$, $3^+D(f\pi)$] do not significantly depend on how many additional weaker states are admitted in the analysis. From this we conclude that Hypothesis I, using 10 waves only, is as suitable as the more complete set of 15 waves of Hypothesis II [the additional small contributions such as, for example, $2^-D(\varepsilon\pi)$, $1^-P(\rho\pi)$, $3^-D(f\pi)$, $1^+P(f\pi)$, etc., seem to take their events mostly from $1^+P(\varepsilon\pi)$].

- In the 1.4-2.0 GeV region a clear enhancement is seen in the $2^-S(f\pi)$ wave at a mass $M = 1.65 \pm 0.03$ GeV with a width $\Gamma = 0.30 \pm 0.05$ GeV. We identify this with the "A_3" peak observed near 1.7 GeV in the missing-mass spectrum and in the 3π effective-mass spectrum, since no other wave shows a peak of comparable strength in this mass region.

- In order to clarify the resonance nature of the A_3 enhancement, we have measured its phase with respect to other partial waves in the same region.

This is possible as the A_3 interferes strongly with all other partial waves. We show in Fig. 9 the phases of $2^-S(f\pi)$ relative to other states. The phases shown have been chosen because they appear to be reasonably well measured. In all cases the relative phase appears to be, within errors, independent of 3π mass. We conclude that the A_3 amplitude does not have the behaviour expected for a Breit-Wigner resonance.

As we have done for the A_1 we comment on the possibility that a real narrow 2^- resonance (A_3^R) is produced at 25-40 GeV/c. We obtain the following upper limits:

$\sigma(A_3^R \to f^0\pi^-$, by s-wave) $\lesssim$ 0.05 μb (1.4 μb) if A_3^R is coherent (incoherent) with the broad $2^-S(f\pi)$ enhancement.

$\sigma(A_3^R \to \rho^0\pi^-$, by p-wave) $\lesssim$ 1.4 μb.

The limits refer in all cases to the final state $\pi^+\pi^-\pi^-$ only.

The polarization density matrix of the A_3 *) (2^-S wave) has been determined by fitting the data in the 3π mass interval 1.5-1.8 GeV with all the spin projections of the 2^-S state, in addition to Hypothesis I. The matrix elements obtained are shown in Table 6: ρ_{00} is largest, close to 1; ρ_{11} and ρ_{1-1} are still measurable; while ρ_{22} and ρ_{2-2} are compatible with zero, in agreement with bubble chamber data at lower energies[4]. The interference term ρ_{10} has the components Re ρ_{10} = 0.18 ± 0.02, Im ρ_{10} = = 0.01 ± 0.03.

The slope b of the differential cross-section $d\sigma/dt$ of the A_3 (2^-S, M = 0) has been determined by fitting the intensity of the 2^-S state (Hypothesis I) of the data in the momentum transfer interval $0.04 < |t| < 0.30$ $(GeV/c)^2$ and in the mass interval $1.5 < m_{3\pi} < 1.8$ GeV with the expression $d\sigma/dt \sim \exp(bt)$, as shown in Fig. 10. A value of b = 9.9 ± ± 1.2 $(GeV/c)^{-2}$ was obtained. For all the remaining events we find b = = 6.4 ± 0.6 $(GeV/c)^{-2}$ in the same interval. It has been checked that the slope is the same for 1.50-1.65 GeV and 1.65-1.80 GeV.

We measure a cross-section of 15.6 ± 1.1 μb for the reaction

$$\pi^- p \to A_3^- p$$
$$\hookrightarrow f^0\pi^-$$
$$\hookrightarrow \pi^+\pi^-$$

*) As discussed in Ref. 1, we assume the same polarization for both $2^-S(f\pi)$ and $2^-P(\rho\pi)$ waves.

in the intervals $1.5 < m_{3\pi} < 1.8$ GeV and $0.04 < |t| < 0.30$ $(GeV/c)^2$ at 40 GeV/c. When integrating the differential cross-section with the above slope over all values of t, we obtain a cross-section of 25.1 ± 1.8 μb with an estimated systematic error of ±3.0 μb. At 25 GeV/c an integrated cross-section of 36 ± 11 μb was measured (see Fig. 14).

5. A POSSIBLE FURTHER RESONANCE

Concerning the question of further resonance effects in our data, we note the presence of a small enhancement in the partial wave $2^+P(f\pi)$ (see Fig. 6). The enhancement has a mass of $M \sim 1.75$ GeV and a width $\Gamma \sim 0.2$ GeV. The relative phases (see Fig. 11) are not inconsistent with a resonance interpretation*). We note, however, that this is a small effect [the ratio $2^+P(f\pi)$ events/total events is 320/3700 events in the bin $m_{3\pi}$ = = 1.7-1.8 GeV] and that -- due to insufficient statistics in this mass region -- we have not been able to include higher partial waves in our analysis. We therefore feel that a definite resonance interpretation of the effect requires additional data.

6. PRODUCTION OF A_1, A_2 AND A_3

In this section we compare the results of this experiment with data from lower energies. We first discuss the energy dependence of A_1, A_2, and A_3 production.

We first note that the polarization of the A_1 is fairly energy-independent. In the momentum transfer interval 0-0.4 $(GeV/c)^2$ an analysis of bubble chamber data at 5, 7, and 7.5 GeV/c yields[3a)], for the most significant density matrix elements in the Gottfried-Jackson system,

$$\rho_{00} = 0.93 \pm 0.02 \ , \quad \mathrm{Re}\ (\rho_{01}) = -0.09 \pm 0.02 \ ,$$

which are very close to the values found at 25 and 40 GeV/c (Table 2).

Figure 12 shows a compilation of integrated cross-sections for A_1 production**) from bubble chamber data between 5 and 25 GeV/c [3a)], and the data of this experiment at 25 and 40 GeV/c.

---

*) The partial-wave analysis of Fig. 11 has been done with the $2^+P(f\pi)$ and the $2^+D(\rho\pi)$ treated as separate waves, i.e. they are not assumed to be fully coherent (as, for example, in the analysis of Fig. 6).

**) The A_1 is defined as the 1^+S state in the 3π mass interval 1.0-1.2 GeV.

Fitting the expression $\sigma \propto p_{inc}^{n}$ to the data we find

$$n = -0.40 \pm 0.06 \ .$$

In the case of the A_2 meson, the polarization density matrix changes with beam momentum. Whereas the analysis of bubble-chamber data at 5, 7, and 7.5 GeV/c [3b)] yields, for the most significant density matrix elements in the Gottfried-Jackson system, in the momentum transfer interval 0-0.4 $(GeV/c)^2$,

$$\rho_{00} = 0.12 \pm 0.04 \ , \quad \rho_{11} + \rho_{1-1} = 0.78 \pm 0.05 \ ;$$

the analysis of this experiment at 40 GeV/c yields (see also Table 4)

$$\rho_{00} = 0.01 \pm 0.02 \ , \quad \rho_{11} + \rho_{1-1} = 0.93 \pm 0.04 \ .$$

In Fig. 13 we therefore show the energy dependence[3c)] of the cross-section[*)] for the polarization states which can be produced by natural and unnatural parity exchange (in the high-energy limit) separately. Fitting the expression $\sigma \propto p_{inc}^{n}$ to the data we find

natural parity exchange: $n = -0.51 \pm 0.05$, $\chi^2 = 8.4/NDF = 9$

unnatural parity exchange: $n = -2.0 \pm 0.3$, $\chi^2 = 0.9/NDF = 4$.

A comparison of the cross-sections for A_3 production[**)] with lower energy data is shown in Fig. 14. When fitting the expression $\sigma \propto p_{inc}^{n}$ for the data above 11 GeV/c, we obtain

$$n = -0.57 \pm 0.21 \ .$$

We obtain additional information on the A_1 and A_2 production from the results about interference between the A_1 and A_2 mesons. From Fig. 15a we see that at 40 GeV/c the intensity of interference between A_1 and A_2 is close to the maximum value allowed by the positivity condition of the density matrix, suggesting the same dependence of both processes on the

---

*) The A_2 is always defined as the 2^+D state in the 3π mass interval 1.2-1.4 GeV.

**) The A_3 is defined as the 2^-S state in the mass interval 1.5-1.8 GeV.

spin variables of the proton. As the differential cross-section of A_1 production does not show any indication of a dip in the forward direction, we guess that both A_1 and A_2 are produced by non-flip amplitudes with respect to the proton spin.

Figure 15b shows the dependence of the relative phase of A_1 and A_2, at the mass of the A_2 meson*), as a function of momentum transfer. In the Regge-pole model this directly measures the difference in slope of the two Regge trajectories exchanged. Within the large errors the phase is independent of momentum transfer.

7. CONCLUSIONS

The partial-wave analysis of the 3π system in the reaction $\pi^- p \to \pi^- \pi^- \pi^+ p$ at 25 and 40 GeV/c has yielded the following results on the A_1, A_2, and A_3 systems:

i) the A_2 can be well described by a Breit-Wigner amplitude;

ii) A_1 and A_3 cannot be described by a Breit- Wigner amplitude;

iii) the energy dependence of A_1, A_2, and A_3 production are similar, and approximately like $p_{inc}^{-0.5}$.

*) Defined as arg (ρ_{ab}), where a = 2^+D1 and b = 1^+S0; the 90° phase of the A_2 propagator has not been subtracted.

REFERENCES

1) Y.M. Antipov et al., The reaction $\pi^- p \to \pi^- \pi^- \pi^+ p$ at 25 and 40 GeV/c, to be submitted to Nuclear Physics B (1973).

2) R. Klanner, Analysis of the reaction $\pi^- p \to \pi^- \pi^- \pi^+ p$ at 25 and 40 GeV/c, CERN-NP Internal Report 73-9 (1973), and Thesis at University of Munich (1973).

3) The program to perform the partial-wave analysis was developed at University of Illinois by G. Ascoli, D.V. Brockway, L. Eisenstein, M.L. Ioffredo, J.D. Hansen, U.E. Kruse and P.F. Schultz. In the following publications the authors applied the method to data of the reaction $\pi^- p \to \pi^- \pi^- \pi^+ p$:
   a) G. Ascoli et al., Phys. Rev. Letters 26, 929 (1971).
   b) D.V. Brockway, Study of the three-pion final state interactions in the reaction $\pi^- p \to \pi^- \pi^- \pi^+ p$ at 5 and 7.5 GeV/c, University of Illinois Report COO-1195-197 (1970).
   c) G. Ascoli et al., Summary of the experimental situation regarding A_1, A_2, and A_3 production, submitted to the 16th Int. Conf. on High-Energy Physics, Batavia 6-13 September 1972.

4) G. Ascoli et al., Spin parity analysis of the A_3, Phys. Rev. D7, 669 (1973).

5) Y.M. Antipov et al., The decay channel $A_2^- \to \eta\pi^-$ in $\pi^- p \to \pi^+ \pi^- \pi^0 \pi^- p$ at 40 GeV/c, to be submitted to Nuclear Physics B (1973).

Table 1

Slope of the differential cross-section ($d\sigma/dt \propto e^{bt}$) and integrated cross-section for production of the 1^+S state. The systematic error is given in parentheses.

	25 GeV/c		40 GeV/c	
$\Delta m_{3\pi}$ (GeV)	b $[(GeV/c)^{-2}]$	$\sigma(A_1)$ (μb)	b $[(GeV/c)^{-2}]$	$\sigma(A_1)$ (μb)
1.0-1.2	12.1 ± 1.1	92 ± 10 (±10)	11.9 ± 1.1	72 ± 5 (±7)
1.2-1.4	8.0 ± 1.0	59 ± 4 (±6)	6.8 ± 0.8	52 ± 3 (±6)

Table 2

A_1 polarization ($J^P = 1^+$, $m_{3\pi} = 1.0$–1.2 GeV)

		$p_{lab} = 25$ GeV/c	$p_{lab} = 40$ GeV/c
"Natural parity exchange"	ρ_{00}	0.94 ± 0.02	0.95 ± 0.02
	$\rho_{11} - \rho_{1-1}$	0.06 ± 0.02	0.05 ± 0.02
	Re (ρ_{10})	-0.15 ± 0.02	-0.13 ± 0.02
	Im (ρ_{10})	0.01 ± 0.03	0.00 ± 0.03
"Unnatural parity exchange"	$\rho_{11} + \rho_{1-1}$	0.00 ± 0.02	0.00 ± 0.02

Table 3

Slope of the differential cross-section ($d\sigma/dt \propto |t|\ e^{bt}$ and integrated cross-section for production of the $A_2(2^+D$, 1.2-1.4 GeV). The systematic error is indicated in parentheses. The momentum transfer interval at 25 GeV/c is too small to determine b from the data. For the extrapolation a value of 8.5 $(GeV/c)^{-2}$ was used.

	$\sigma(A_2)$ (μb)	b $[(GeV/c)^{-2}]$
25 GeV/c	15 ± 3(±2)	
40 GeV/c	18 ± 2(±2)	8.6 ± 1.2

Table 4

A_2 polarization ($J^P = 2^+$, $m_{3\pi} = 1.2$-1.4 GeV)

"Natural parity exchange"	$\rho^0\pi^-$ $p_{lab} = 25$ GeV/c	$\rho^0\pi^-$ $p_{lab} = 40$ GeV/c	$\eta^0\pi^-$ $p_{lab} = 40$ GeV/c
$\rho_{11} + \rho_{1-1}$	0.90 ± 0.04	0.93 ± 0.04	0.97 ± 0.06
$\rho_{22} - \rho_{2-2}$	0.06 ± 0.05	0.07 ± 0.04	0.03 ± 0.05
Re (ρ_{21})	0.12 ± 0.04	0.10 ± 0.03	0.02 ± 0.07
Im (ρ_{21})	0.01 ± 0.12	-0.03 ± 0.03	-
Trace	0.96 ± 0.04	0.99 ± 0.04	1.00 ± 0.07
"Unnatural parity exchange"			
Trace	0.04 ± 0.04	0.01 ± 0.04	0.00 ± 0.07

Table 5

Sets of partial waves used in the analysis of the A_3 region (see Fig. 6)

Decay mode	$\epsilon\pi$			$\rho\pi$							$f\pi$				
$J^P\ell$	0^-S	1^+P	2^-D	1^+S	0^-P	1^-P	2^-P	1^+D	2^+D	3^+D	2^-S	1^+P	2^+P	3^+P	3^-D
M	0	0	0	0	0	0	0	0	1	0	0	0	1	0	1
Hypothesis I (-•-)	x	x		x	x		x		x	x	x		x	x	
Hypothesis II (-o-)	x	x	x	x	x	x	x	x	x	x	x	x	x	x	x

Hypothesis I coincides with the choice of Ascoli et al. given in Ref. 4.

Table 6

A_3 polarization ($J^P = 2^-$, $m_{3\pi}$ = 1.5-1.8 GeV) (40 GeV/c data)

"Natural parity exchange"		
ρ_{00}	0.88 ± 0.04	
$\rho_{11} - \rho_{1-1}$	0.10 ± 0.02	
$\rho_{22} + \rho_{2-2}$	0.01 ± 0.02	
ρ_{10}	0.19 ± 0.02	+i (0.02 ± 0.03)
ρ_{20}	-0.06 ± 0.02	+i (0.01 ± 0.03)
ρ_{21}	-0.02 ± 0.01	+i (-0.01 ± 0.03)
Trace	0.99 ± 0.02	
"Unnatural parity exchange"		
Trace	0.01 ± 0.02	

Figure captions

Fig. 1 : Intensities of different partial waves and interference phases in the A_1 region for the reaction $\pi^- p \to \pi^- \pi^- \pi^+ p$:

a) 25 GeV/c [combination of runs in the momentum transfer intervals Δt = 0.10-0.30 $(GeV/c)^2$ and 0.17-0.30 $(GeV/c)^2$];

b) 40 GeV/c data [Δt = 0.04-0.30, 0.10-0.30 and 0.17-0.30 $(GeV/c)^2$];

c) 25 GeV/c and 40 GeV/c data combined.

Fig. 2 : Differential cross-section for the reaction $\pi^- p \to A_1^- p$ at 25 and 40 GeV/c in the mass intervals 1.0-1.2 GeV and 1.2-1.4 GeV.

Fig. 3 : a) and b) Polarization of the A_1 system. The dependence of the rotation angle θ, between the Gottfried-Jackson system and the system where the A_1 is in a pure M = 0 state, is shown as a function of momentum transfer t. θ_c is the angle between the direction of the incident particle and the direction opposite to the recoil proton in the 3π centre-of-mass system (crossing angle).

Fig. 4 : a) Intensity of the 2^+D wave at 40 GeV/c versus 3π mass.

b) Interference phase of the 2^+D wave with the 1^+ waves versus 3π mass.

Fig. 5 : Differential cross-section for A_2 production at 25 and 40 GeV/c in the 3π mass interval 1.2-1.4 GeV.

Fig. 6 : Partial wave analysis of the "A_3 region" for the reaction $\pi^- p \to \pi^- \pi^- \pi^+ p$ at 40 GeV/c. For a detailed description of the different sets of partial waves (hypotheses) used, see Table 5 and the text. For completeness we have also included the 1.0-1.4 mass region for hypothesis I.

Fig. 7 : Comparison of the data measured at 40 GeV/c (histogram) with the partial wave fit (smooth curve) in the 3π mass interval 1.6-1.7 GeV:

a) $m^2_{\pi^+\pi^-}$ (2 combinations per event);

b) $m^2_{\pi^-\pi^-}$.

Fig. 8 : Comparison of the data measured at 40 GeV/c (histogram) with the partial wave fit (smooth curve) in the 3π mass interval 1.6-1.7 GeV. Distribution of the Euler-angles of the 3π system measured from the Gottfried-Jackson axes:

a) α azimuth of the π^+;

b) $\cos\beta$ polar angle of the π^+;

c) γ, angle between the decay plane and the plane formed by π^-_{in} and π^+_{out}.

Fig. 9 : Intensity of the $2^-S(f\pi)$ partial wave and interference in the A_3 region, measured at 40 GeV/c.

Fig. 10 : $|t|$-dependence of the A_3 (2^-S wave, M = 0). The slope parameter $b = 9.9 \pm 1.2$ was determined by a fit with exp (bt). The upper points are for all remaining events in the same mass interval 1.50-1.80 GeV. They have a slope of $b = 6.4 \pm 0.6$. The data are taken at $p_{inc} = 40$ GeV/c.

Fig. 11 : The $2^+P(f\pi)$ partial wave in the reaction $\pi^-p \to \pi^-\pi^-\pi^+p$ at 40 GeV/c and $0.04 < |t| < 0.33$ $(GeV/c)^2$:

a) intensity as a function of 3π mass;

b) the phase difference of $2^+P(f\pi)$ relative to $2^-P(\rho\pi)$, $1^+P(\rho\pi)$, and $1^+S(\rho\pi)$.

Fig. 12 : Energy dependence of the integrated A_1 cross-section $\sigma(A_1)$ for the 3π mass interval 1.0-1.2 GeV. The solid line is a fit $\sigma(A_1) \propto p^n_{inc}$ with $n = -0.40 \pm 0.06$.

Fig. 13 : Energy dependence of the natural $\sigma_N(A_2)$ and unnatural $\sigma_U(A_2)$ parity exchange contributions to the A_2 cross-section in the 3π mass interval 1.2-1.4 GeV. The solid lines are fits $\sigma(A_2) \propto p_{inc}^n$ with $n_N = -0.51 \pm 0.05$ and $n_U = -2.0 \pm 0.3$.

Fig. 14 : Energy dependence of the integrated A_3 cross-section $\sigma(A_3)$ for the 3π mass interval 1.5-1.8 GeV. The solid line is a fit $\sigma(A_3) \propto p_{inc}^n$ with $n = -57 \pm 0.21$.

Fig. 15 : Interference between A_1 and A_2 at 40 GeV/c.

a) Coherence between A_1 and A_2 versus momentum transfer.

b) Interference phase between A_1 and A_2 at the centre of the A_2 versus momentum transfer.

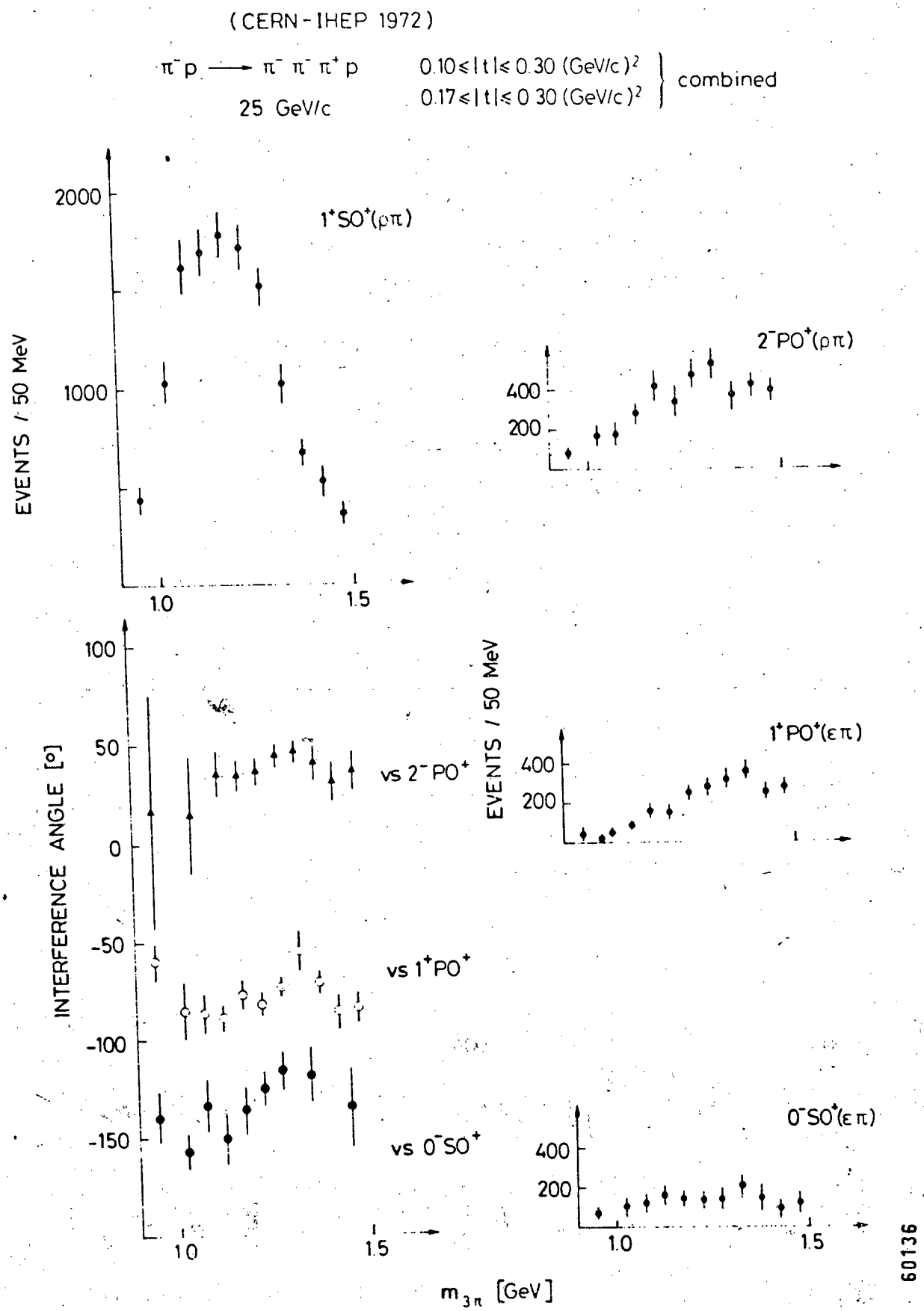
(CERN-IHEP 1972)
π⁻p → π⁻ π⁻ π⁺ p
25 GeV/c
0.10 ≤ |t| ≤ 0.30 (GeV/c)²
0.17 ≤ |t| ≤ 0.30 (GeV/c)²
combined
1⁺SO⁺(ρπ)
2⁻PO⁺(ρπ)
1⁺PO⁺(επ)
0⁻SO⁺(επ)
EVENTS / 50 MeV
INTERFERENCE ANGLE [°]
vs 2⁻PO⁺
vs 1⁺PO⁺
vs 0⁻SO⁺
m3π [GeV]
60136

Fig. 1a

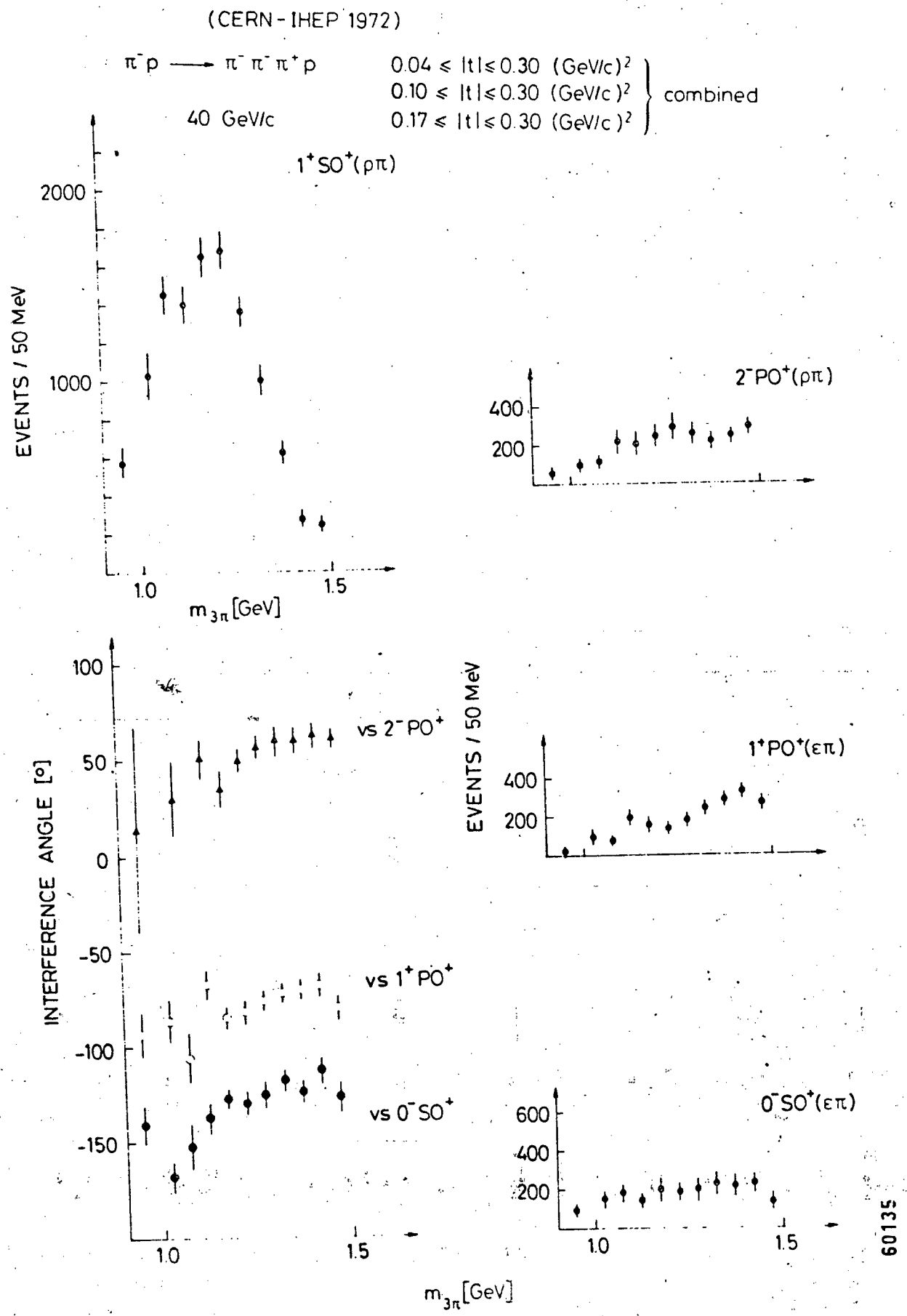
(CERN - IHEP 1972)
π⁻p → π⁻π⁻π⁺p
40 GeV/c
0.04 ≤ |t| ≤ 0.30 (GeV/c)²
0.10 ≤ |t| ≤ 0.30 (GeV/c)²
0.17 ≤ |t| ≤ 0.30 (GeV/c)²
combined
1⁺SO⁺(ρπ)
EVENTS / 50 MeV
2000
1000
1.0
1.5
m3π [GeV]
2⁻PO⁺(ρπ)
400
200
INTERFERENCE ANGLE [°]
100
50
0
-50
-100
-150
vs 2⁻PO⁺
vs 1⁺PO⁺
vs 0⁻SO⁺
1⁺PO⁺(επ)
0⁻SO⁺(επ)
600
60135

Fig. 1b

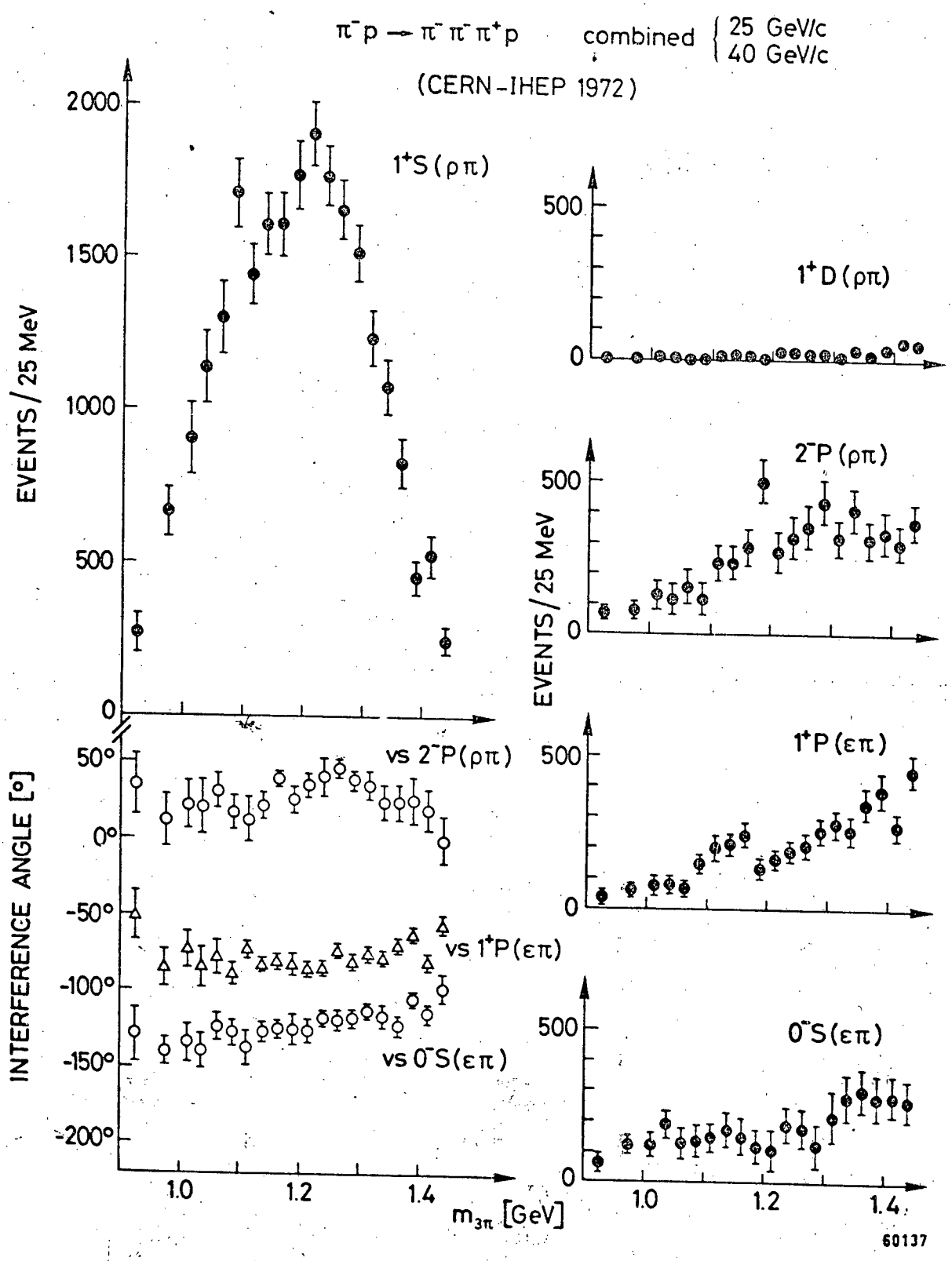
π⁻p → π⁻π⁻π⁺p
combined
25 GeV/c
40 GeV/c
(CERN-IHEP 1972)
1⁺S(ρπ)
1⁺D(ρπ)
2⁻P(ρπ)
1⁺P(επ)
0⁻S(επ)
EVENTS / 25 MeV
INTERFERENCE ANGLE [°]
vs 2⁻P(ρπ)
vs 1⁺P(επ)
vs 0⁻S(επ)
m3π [GeV]
60137

Fig. 1c

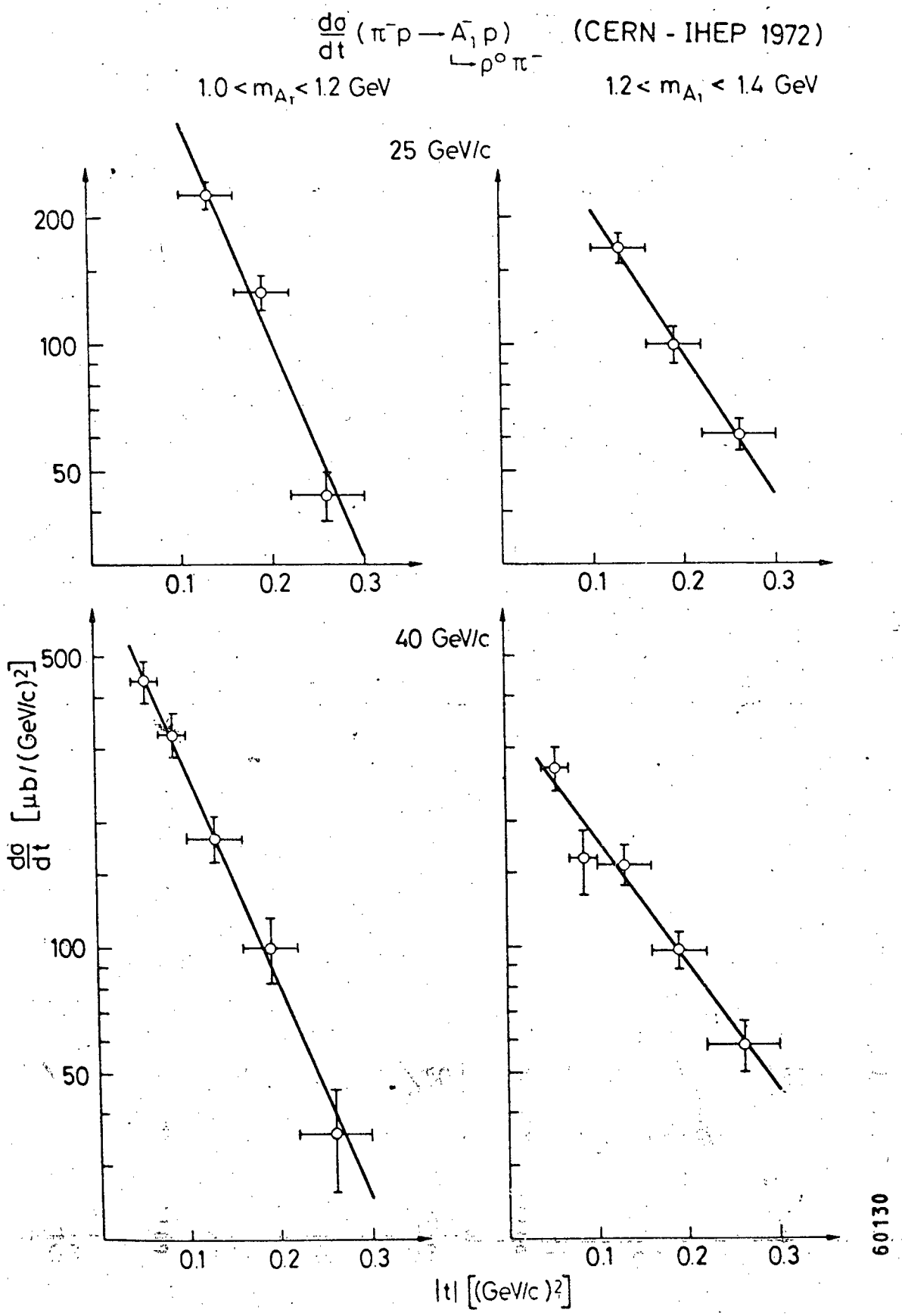
$\frac{d\sigma}{dt}(\pi^- p \to A_1^- p)$ (CERN - IHEP 1972)
$\hookrightarrow \rho^0 \pi^-$
$1.0 < m_{A_1} < 1.2$ GeV
$1.2 < m_{A_1} < 1.4$ GeV
25 GeV/c
40 GeV/c
200
100
50
500
100
50
0.1
0.2
0.3
$\frac{d\sigma}{dt}$ [μb/(GeV/c)²]
|t| [(GeV/c)²]
60130

Fig. 2

(CERN - IHEP 1972)

40 GeV $\pi^- p \longrightarrow \pi^- \pi^- \pi^+ p$

ROTATION ANGLE FROM G.J. SYSTEM TO D-H SYSTEM

FOR 1^+-WAVE

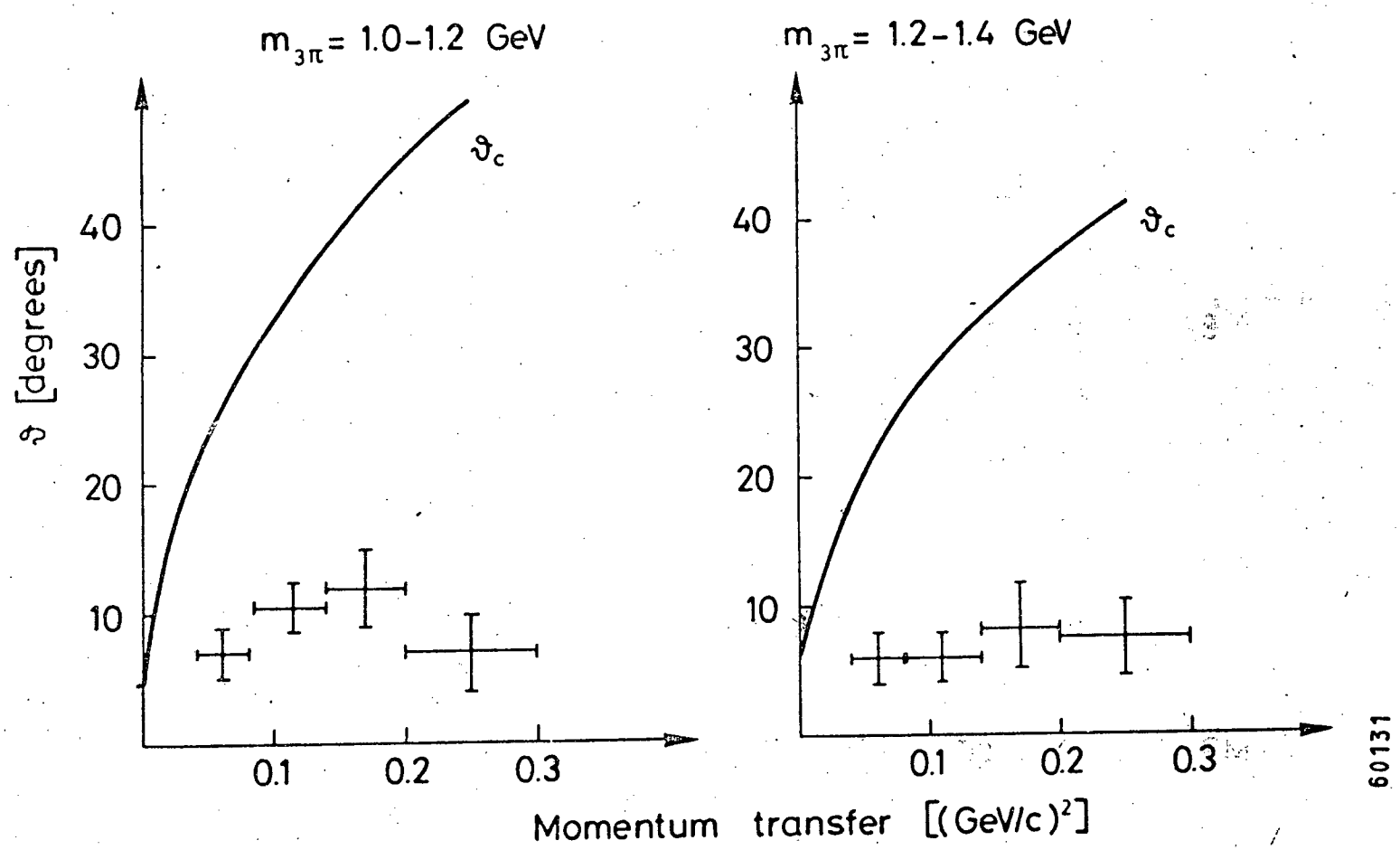

Fig. 3

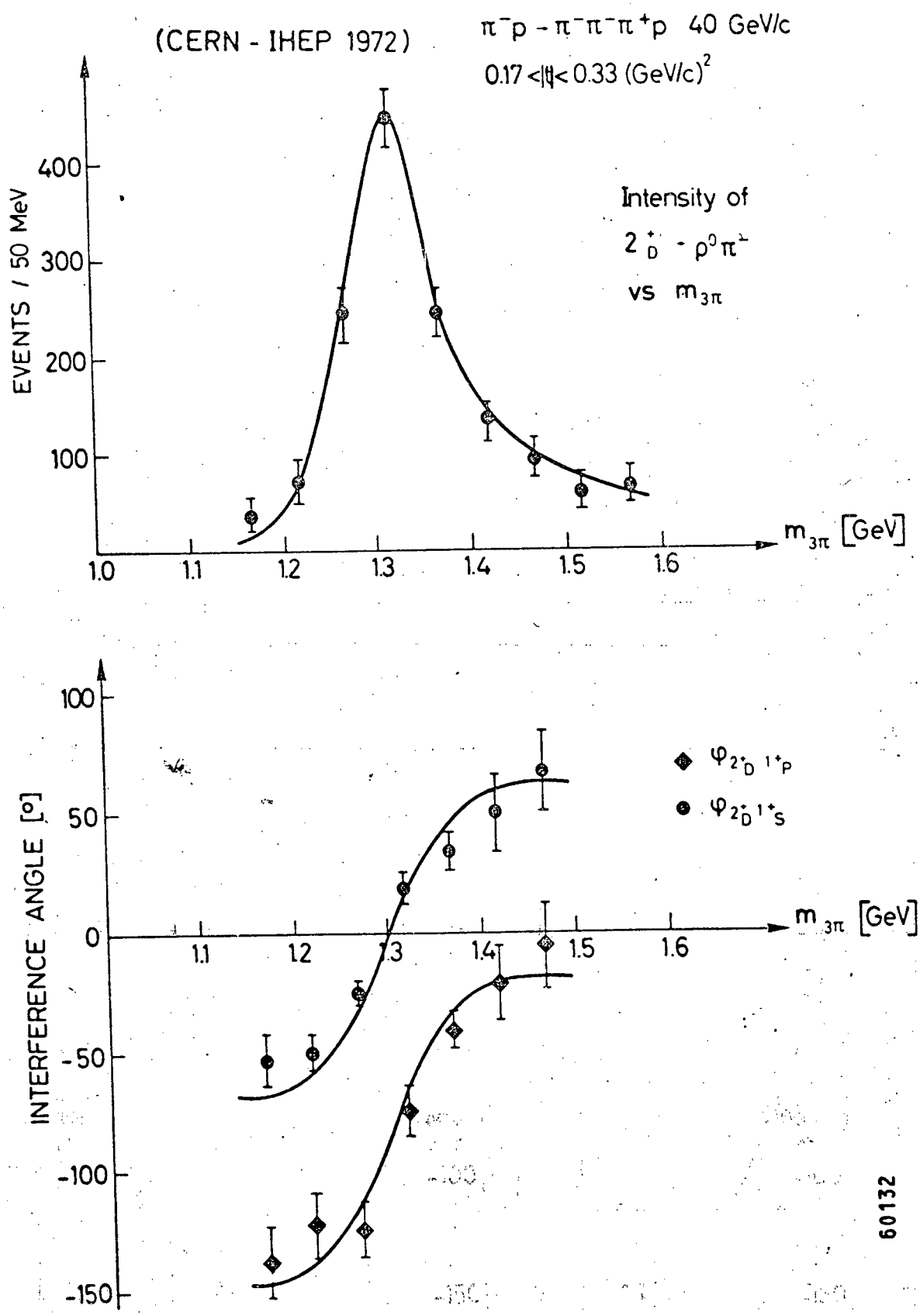
(CERN - IHEP 1972)
$\pi^- p \to \pi^- \pi^- \pi^+ p$ 40 GeV/c
$0.17 < |t| < 0.33$ (GeV/c)^2
Intensity of
$2^+_D - \rho^0 \pi^-$
vs $m_{3\pi}$
EVENTS / 50 MeV
400
300
200
100
1.0
1.1
1.2
1.3
1.4
1.5
1.6
$m_{3\pi}$ [GeV]
INTERFERENCE ANGLE [°]
100
50
0
-50
-100
-150
$\varphi_{2^+_D 1^+_P}$
$\varphi_{2^+_D 1^+_S}$
60132

Fig. 4

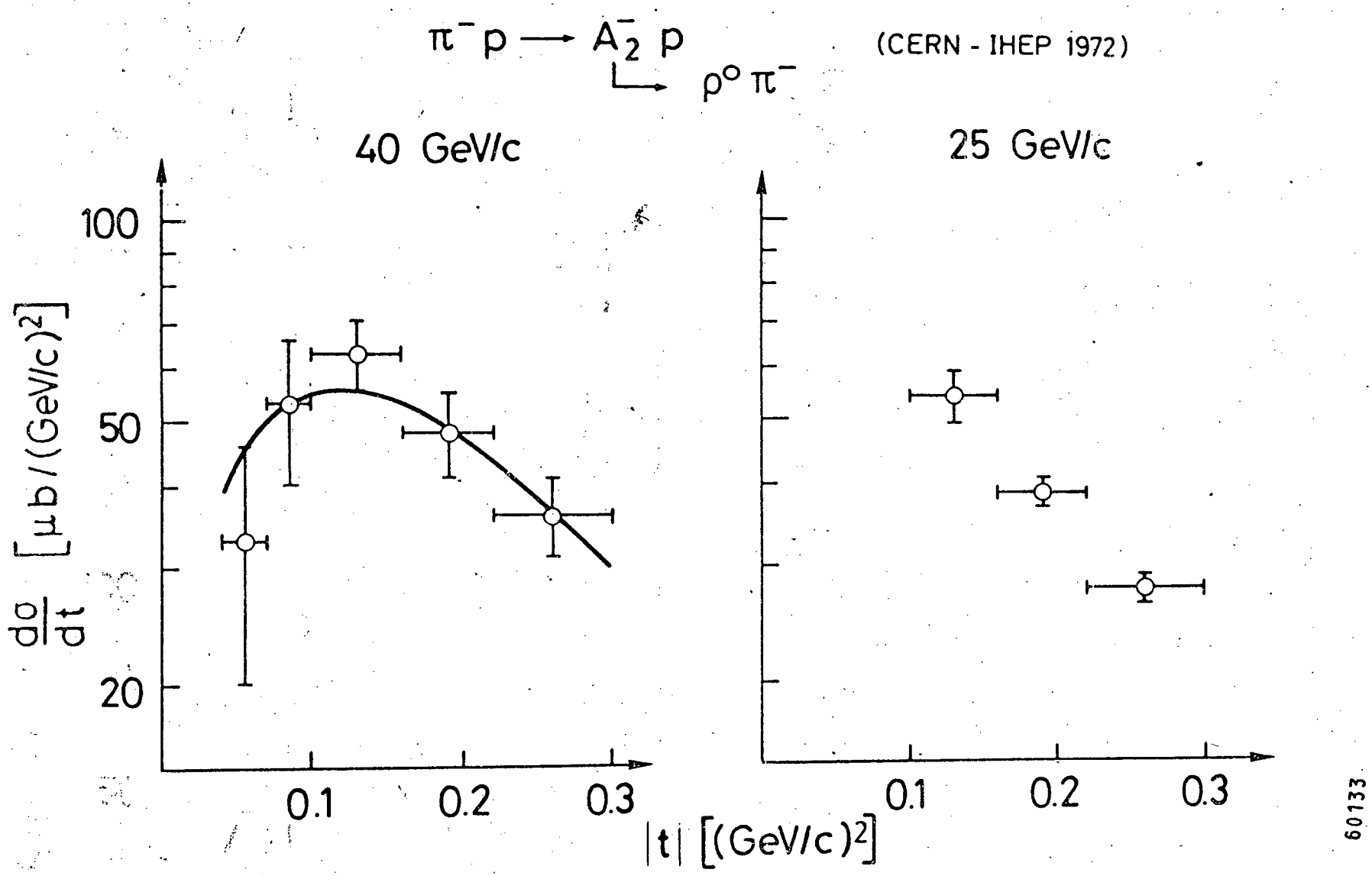
$\pi^- p \longrightarrow A_2^- p$
$\hookrightarrow \rho^0 \pi^-$
(CERN - IHEP 1972)
40 GeV/c
25 GeV/c
100
50
20
$\frac{d\sigma}{dt}$ [μb/(GeV/c)²]
0.1
0.2
0.3
|t| [(GeV/c)²]
60133

Fig. 5

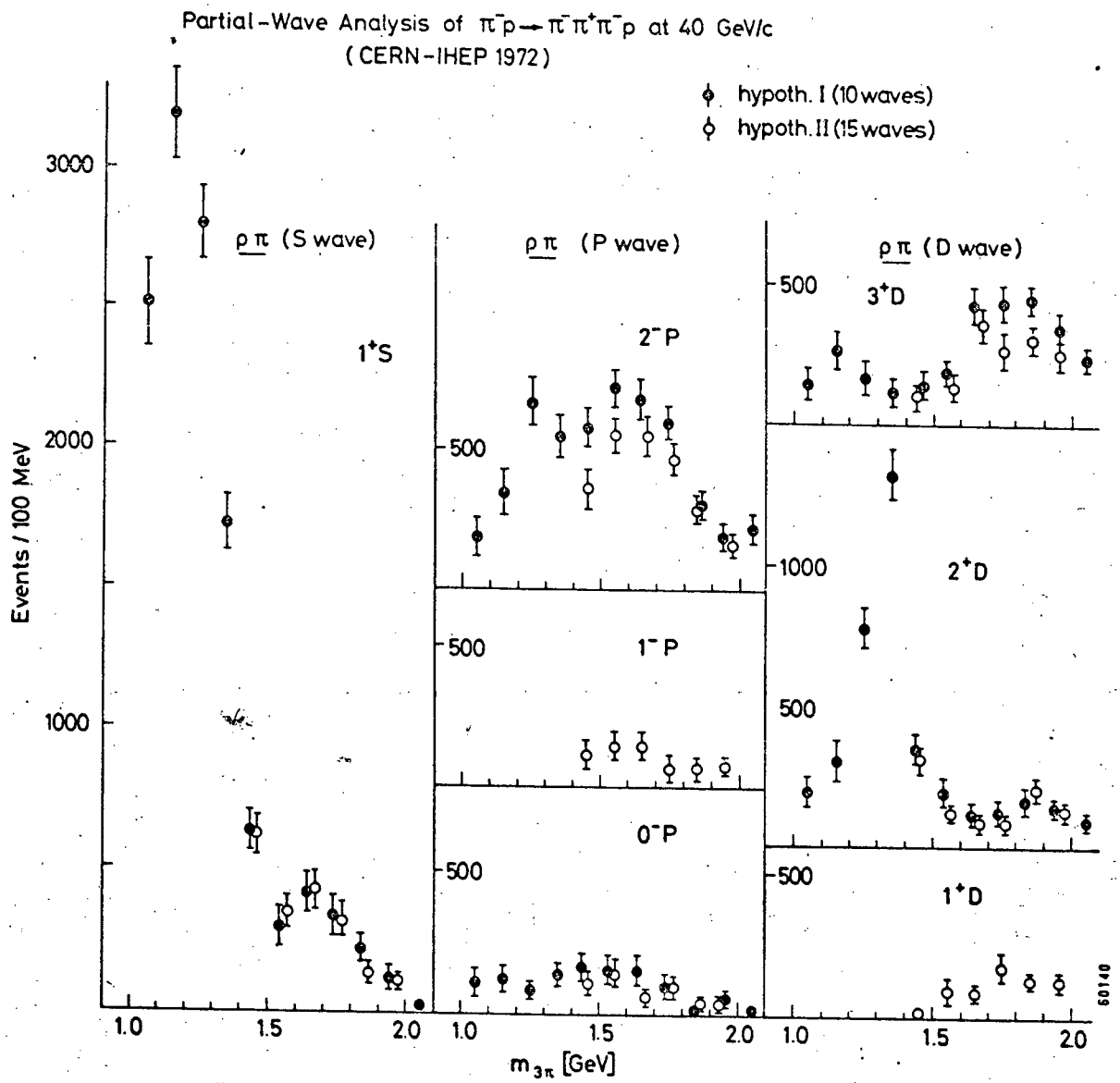
Partial-Wave Analysis of $\pi^- p \to \pi^- \pi^+ \pi^- p$ at 40 GeV/c
(CERN-IHEP 1972)
hypoth. I (10 waves)
hypoth. II (15 waves)
ρπ (S wave)
ρπ (P wave)
ρπ (D wave)
1^+S
2^-P
1^-P
0^-P
3^+D
2^+D
1^+D
Events / 100 MeV
3000
2000
1000
500
1000
1.0
1.5
2.0
$m_{3\pi}$ [GeV]
60140

Fig. 6a

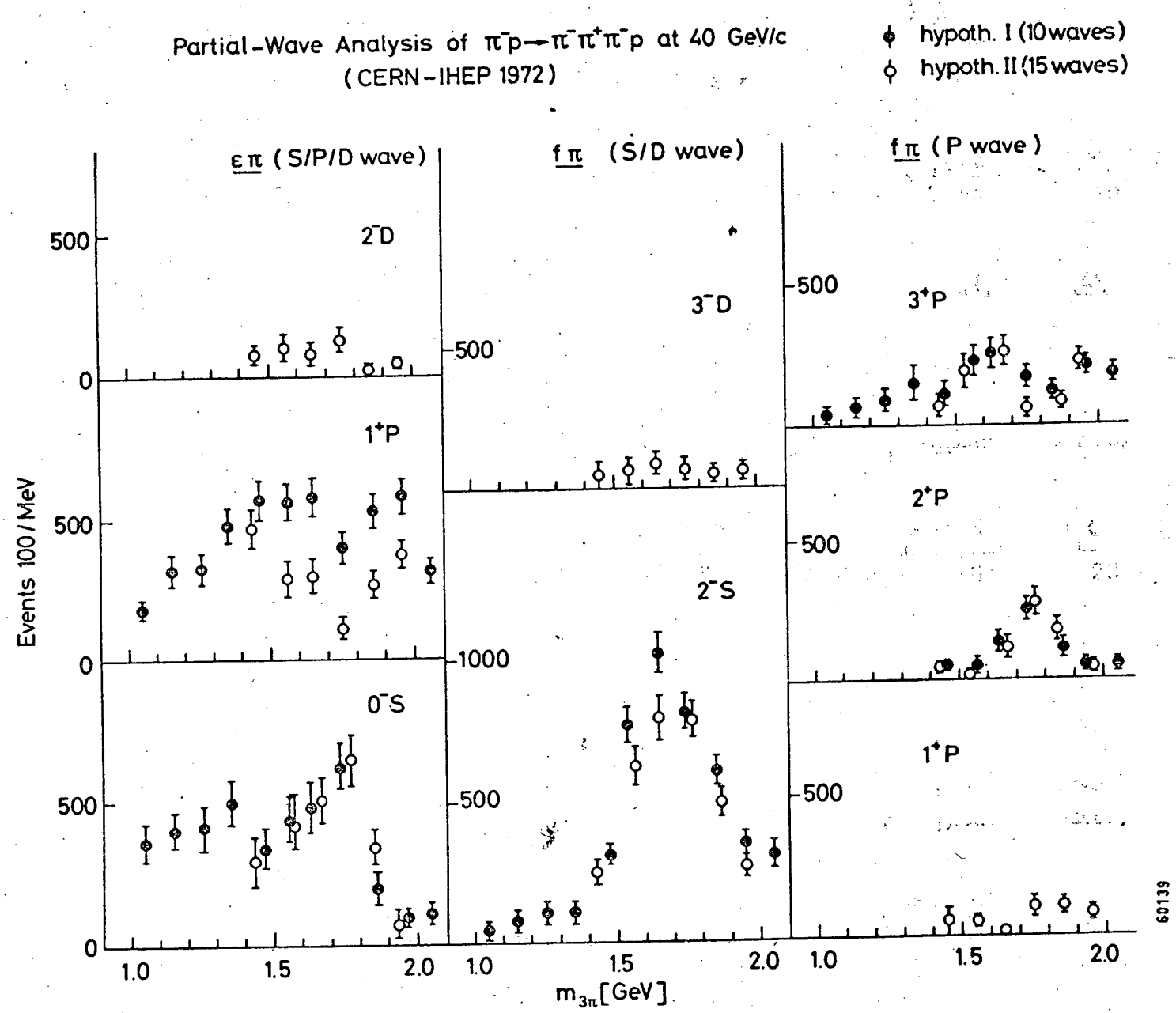
Partial-Wave Analysis of $\pi^- p \to \pi^- \pi^+ \pi^- p$ at 40 GeV/c
(CERN-IHEP 1972)
hypoth. I (10 waves)
hypoth. II (15 waves)
ε π (S/P/D wave)
f π (S/D wave)
f π (P wave)
2^-D
3^-D
3^+P
1^+P
2^-S
2^+P
0^-S
1^+P
Events 100/MeV
500
1000
0
1.0
1.5
2.0
$m_{3\pi}$[GeV]
60139

Fig. 6b

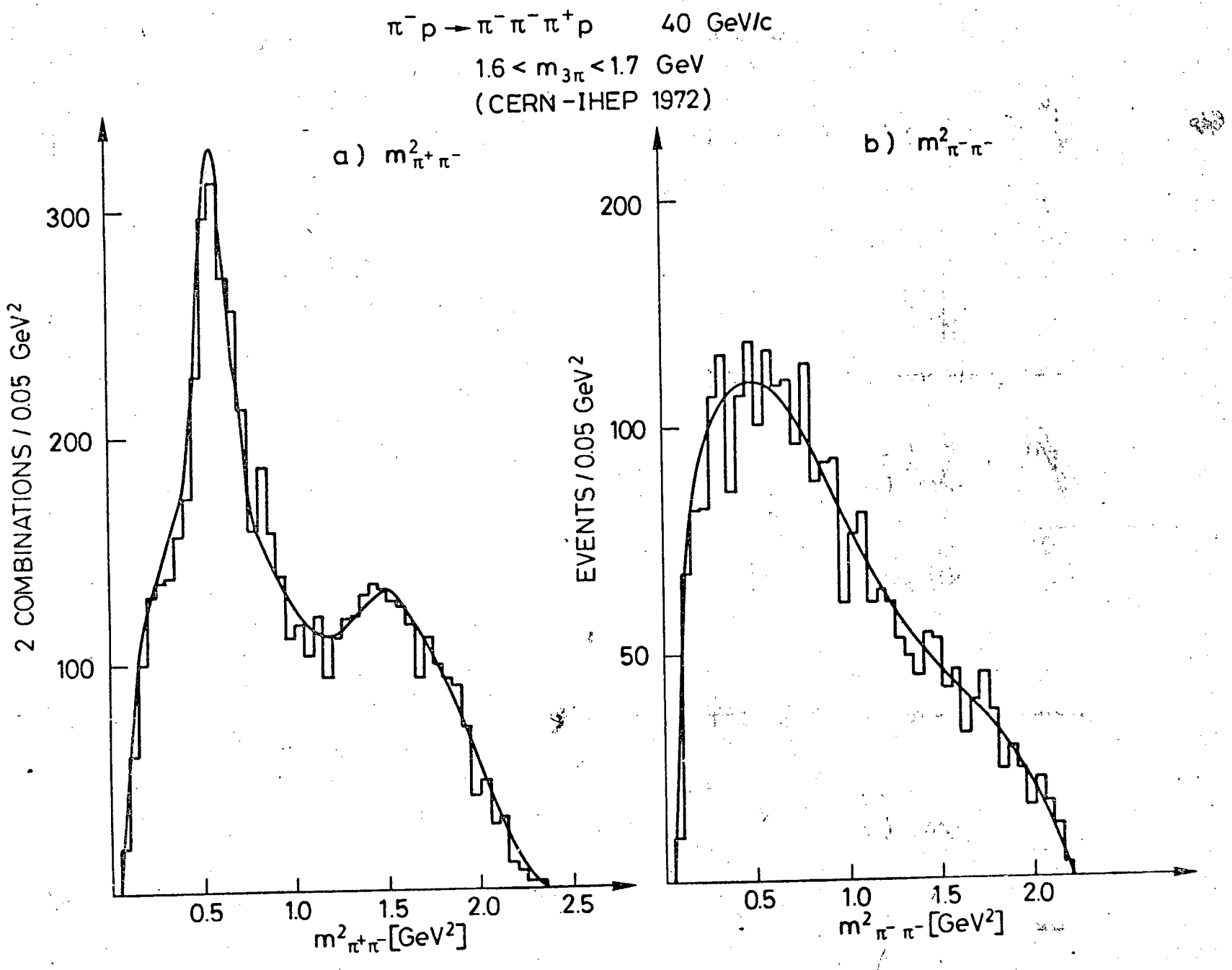
$\pi^- p \to \pi^- \pi^- \pi^+ p$ 40 GeV/c
$1.6 < m_{3\pi} < 1.7$ GeV
(CERN-IHEP 1972)
a) $m^2_{\pi^+\pi^-}$
b) $m^2_{\pi^-\pi^-}$
2 COMBINATIONS / 0.05 GeV^2
EVENTS / 0.05 GeV^2
300
200
100
50
0.5
1.0
1.5
2.0
2.5
$m^2_{\pi^+\pi^-}$ [GeV^2]
$m^2_{\pi^-\pi^-}$ [GeV^2]

Fig. 7

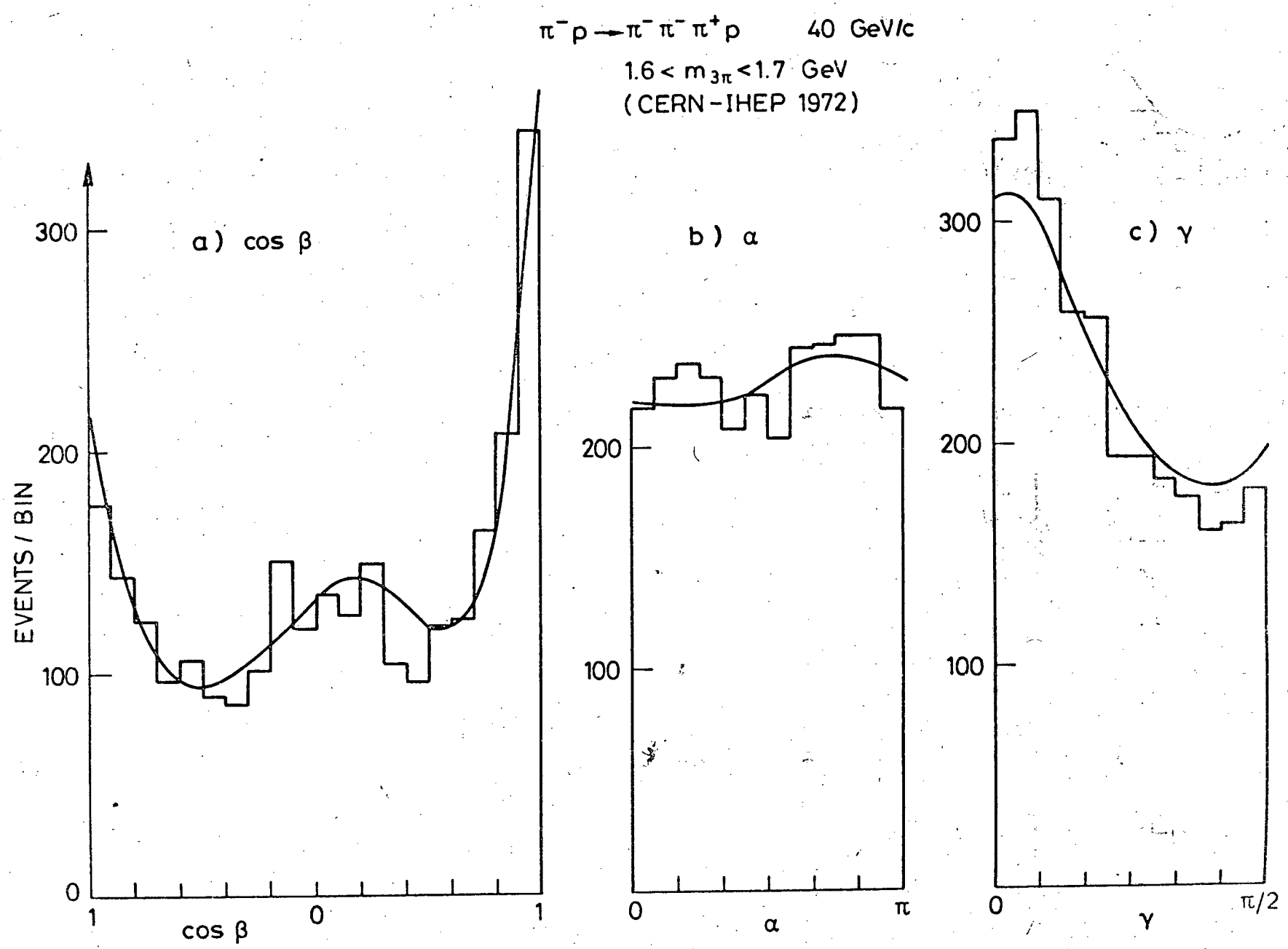
π⁻p → π⁻π⁻π⁺p 40 GeV/c
1.6 < m3π < 1.7 GeV
(CERN-IHEP 1972)
a) cos β
b) α
c) γ
EVENTS / BIN
300
200
100
0
1
0
1
cos β
0
α
π
0
γ
π/2

Fig. 8

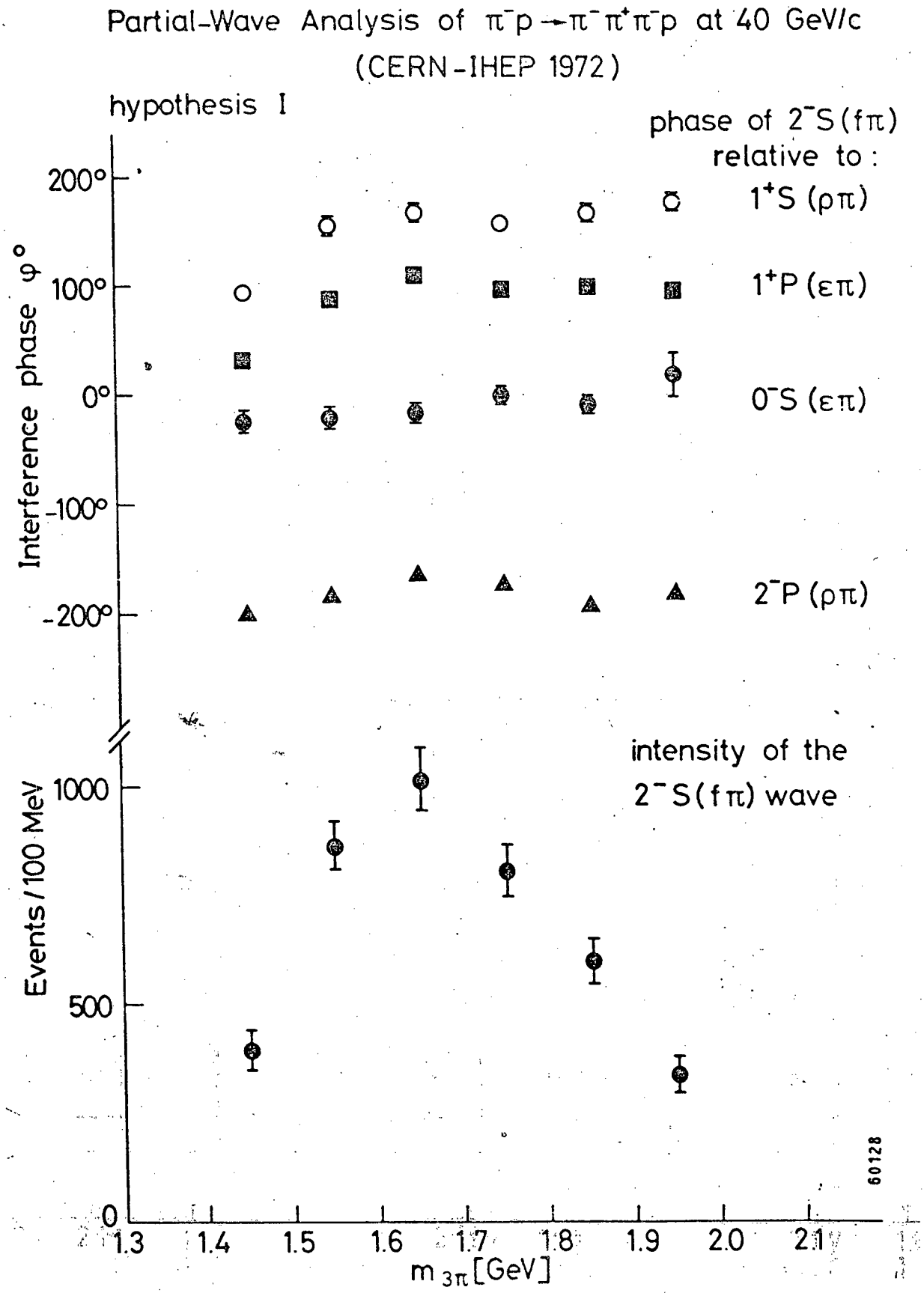
Partial-Wave Analysis of $\pi^- p \to \pi^- \pi^+ \pi^- p$ at 40 GeV/c
(CERN-IHEP 1972)
hypothesis I
phase of $2^-S(f\pi)$ relative to:
$1^+S(\rho\pi)$
$1^+P(\varepsilon\pi)$
$0^-S(\varepsilon\pi)$
$2^-P(\rho\pi)$
Interference phase $\varphi°$
200°
100°
0°
-100°
-200°
intensity of the $2^-S(f\pi)$ wave
Events / 100 MeV
1000
500
0
1.3
1.4
1.5
1.6
1.7
1.8
1.9
2.0
2.1
$m_{3\pi}$ [GeV]
60128

Fig. 9

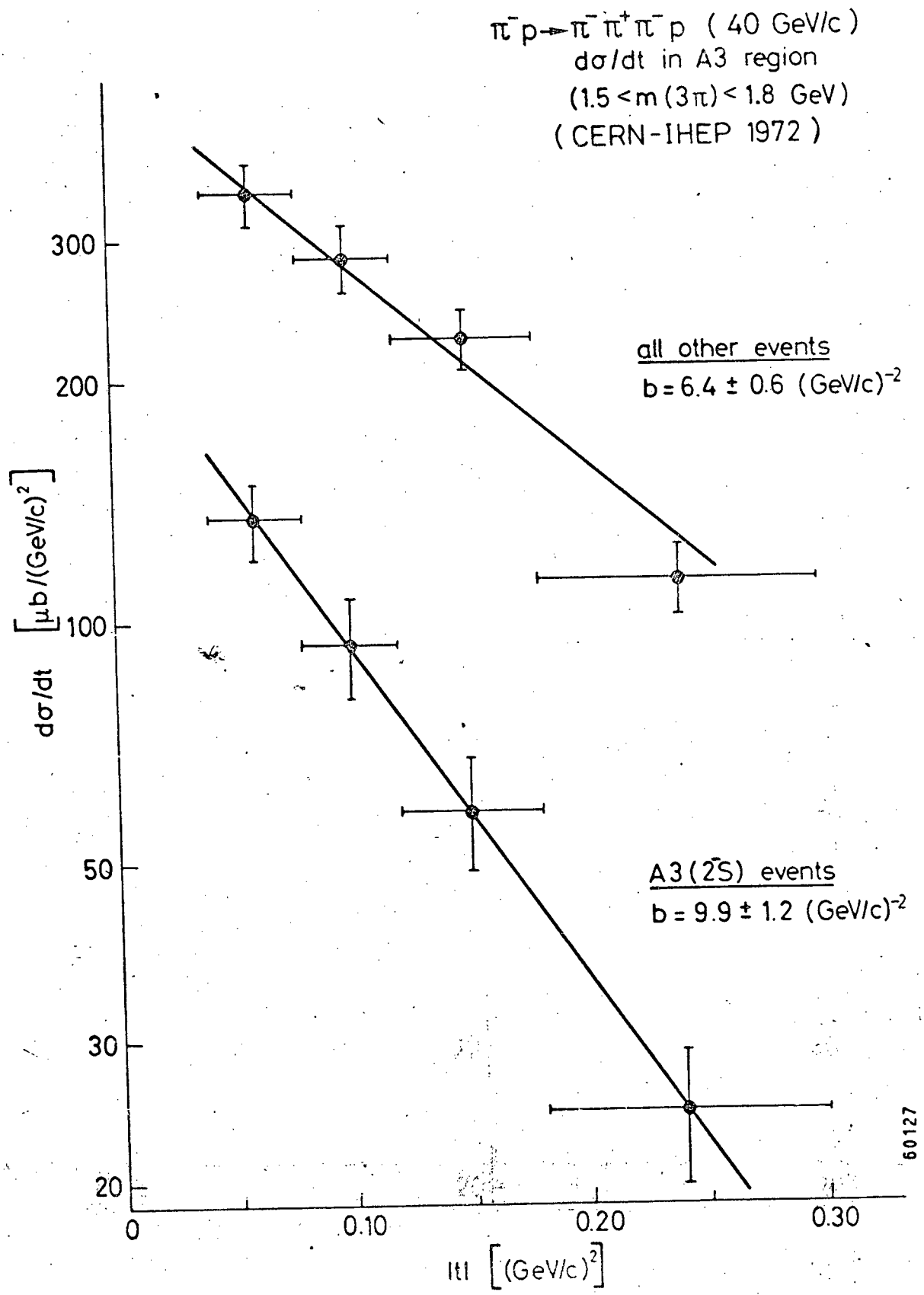
π⁻p→π⁻π⁺π⁻p (40 GeV/c)
dσ/dt in A3 region
(1.5 < m(3π) < 1.8 GeV)
(CERN-IHEP 1972)
all other events
b = 6.4 ± 0.6 (GeV/c)⁻²
A3(2⁻S) events
b = 9.9 ± 1.2 (GeV/c)⁻²
dσ/dt [μb/(GeV/c)²]
300
200
100
50
30
20
0
0.10
0.20
0.30
|t| [(GeV/c)²]
60127

Fig. 10

Partial-Wave Analysis of $\pi^- p \rightarrow \pi^- \pi^+ \pi^- p$ at 40 GeV/c

$(0.04 < |t| < 0.33 (\mathrm{GeV/c})^2)$

The $2^+ P (f\pi)$ Wave (CERN-IHEP 1972)

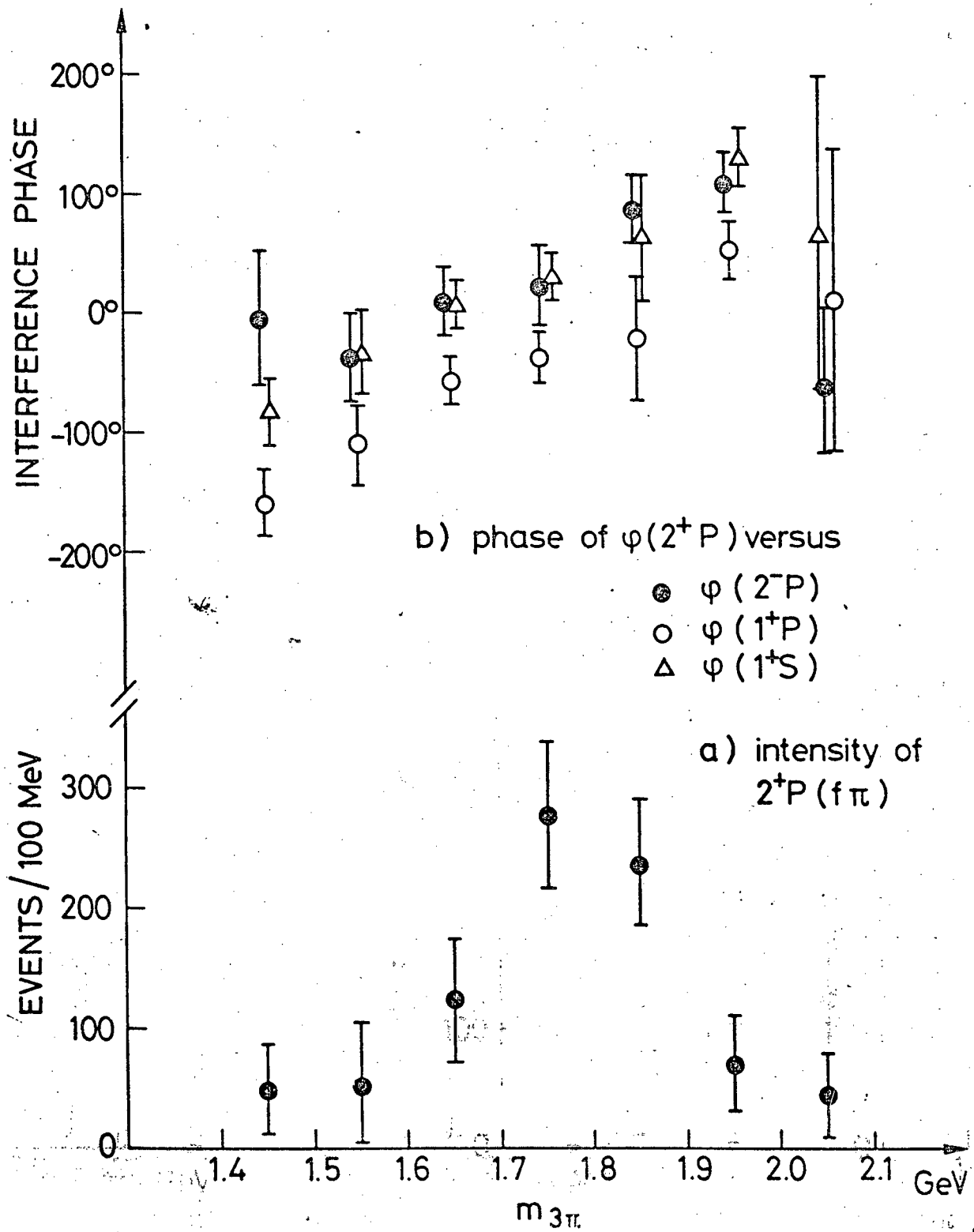

Fig. 11

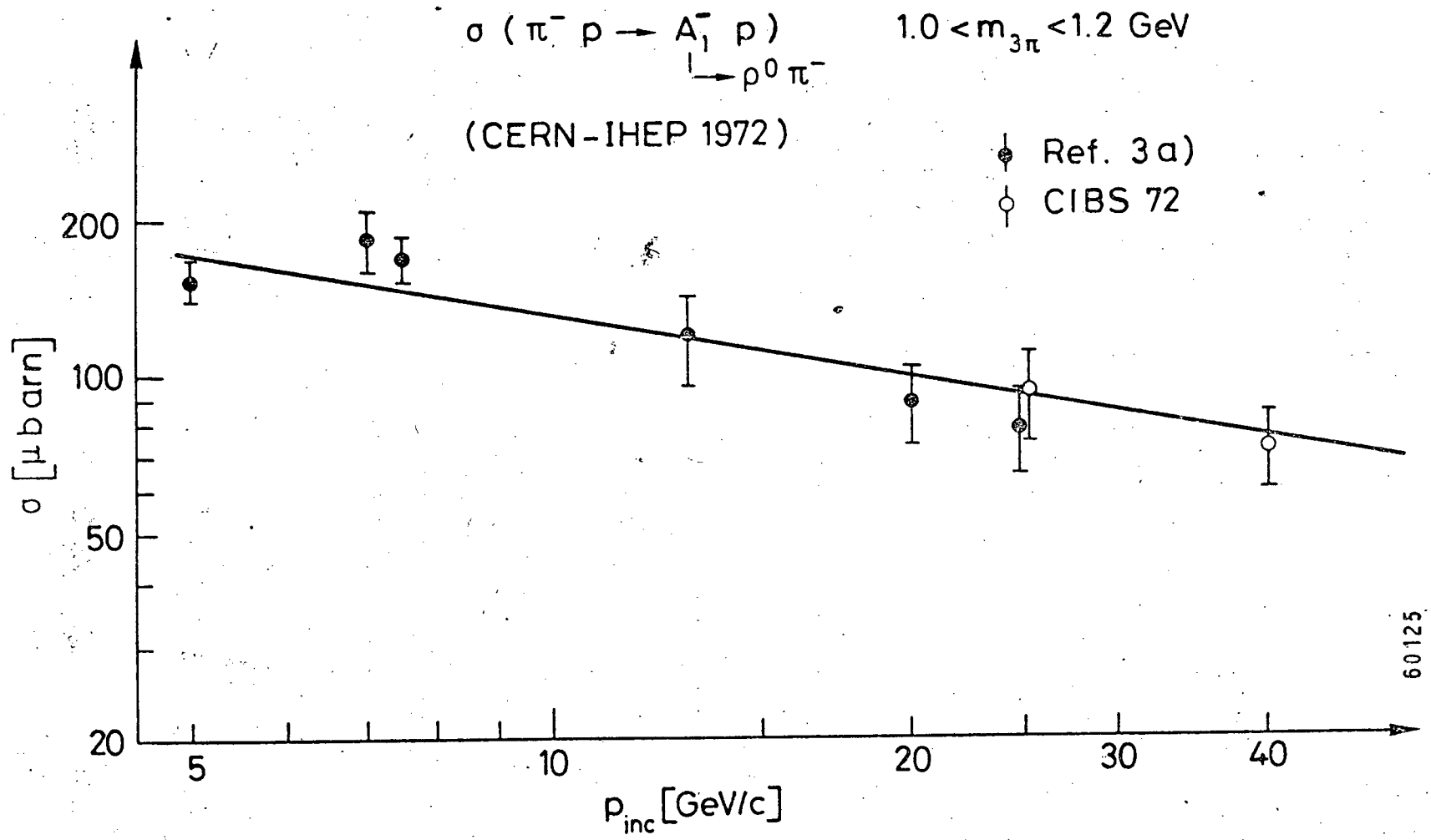
σ (π⁻ p → A₁⁻ p)
↳ ρ⁰ π⁻
1.0 < m₃π < 1.2 GeV
(CERN-IHEP 1972)
Ref. 3a)
CIBS 72
σ [μbarn]
200
100
50
20
5
10
20
30
40
p_inc [GeV/c]
60125

Fig. 12

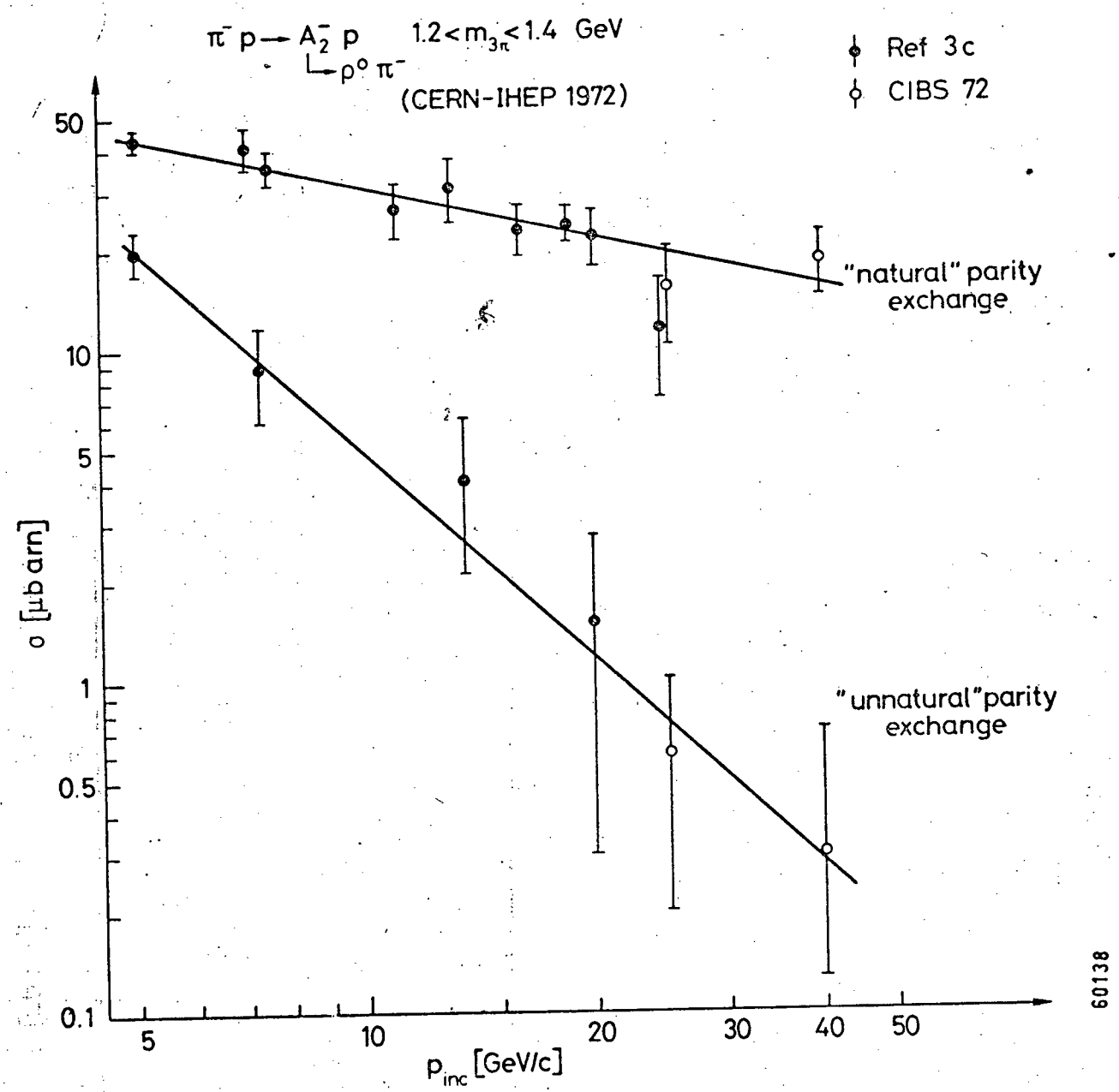
$\pi^- p \rightarrow A_2^- p$ $1.2 < m_{3\pi} < 1.4$ GeV
$\hookrightarrow \rho^0 \pi^-$
(CERN-IHEP 1972)
Ref 3c
CIBS 72
"natural" parity exchange
"unnatural" parity exchange
σ [μbarn]
50
10
5
1
0.5
0.1
5
10
20
30
40
50
p_{inc} [GeV/c]
60138

Fig. 13

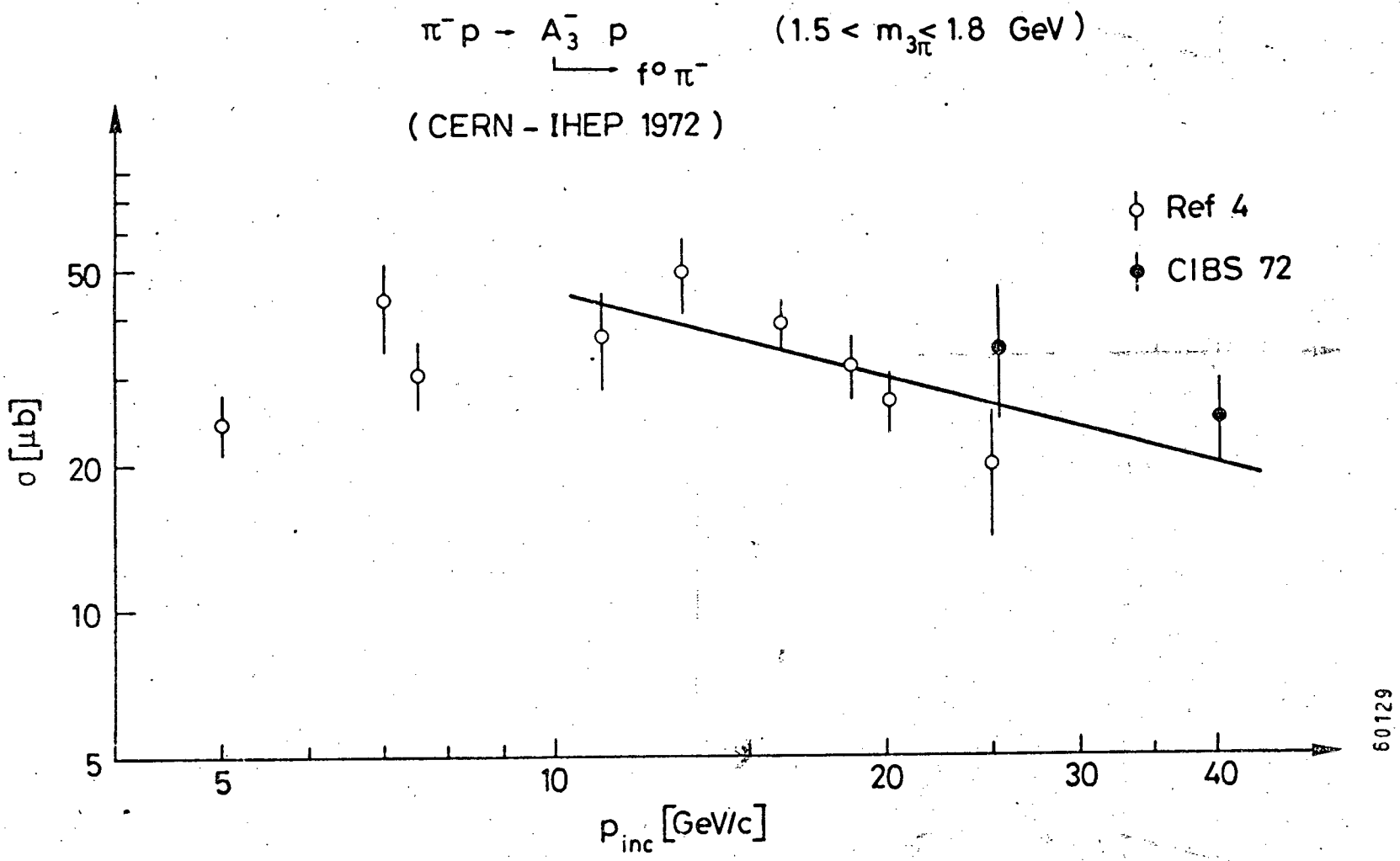
π⁻p → A₃⁻ p
f°π⁻
(1.5 < m₃π < 1.8 GeV)
(CERN - IHEP 1972)
Ref 4
CIBS 72
σ [μb]
50
20
10
5
5
10
20
30
40
p_inc [GeV/c]
60129

Fig. 14

(CERN - IHEP 1972)

$\pi^- p \longrightarrow \pi^- \pi^- \pi^+ p$

INTERFERENCE OF 1^+S AND 2^+D STATES

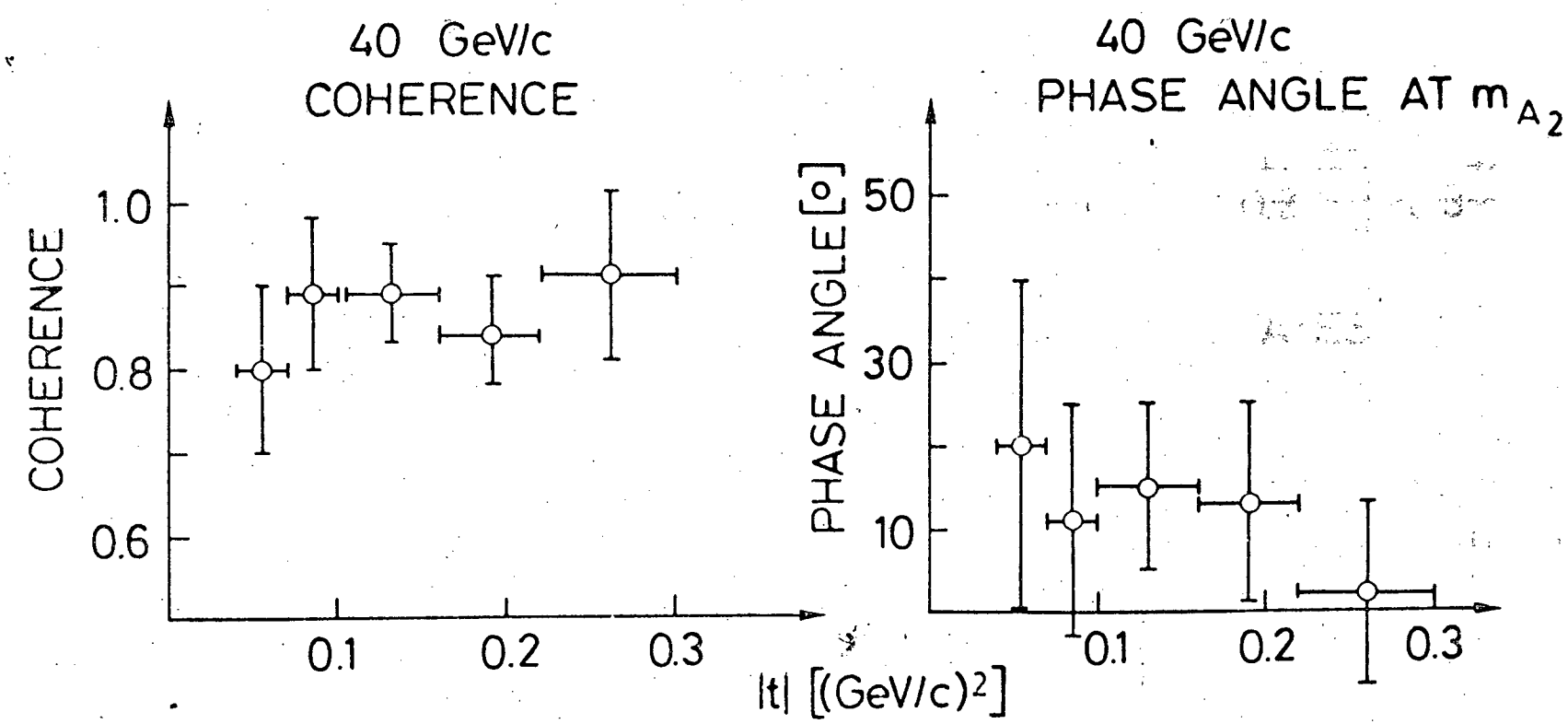

Fig. 15

60134